Letter

Narrowing Linewidth of Wavelength-Swept Active Mode Locking Laser Based on Cross Gain Modulation

Se Jin Park [1,†], Gyeong Hun Kim [1,†], Hwi Don Lee [2], Chang-Seok Kim [1,*] and Minsik Jo [3,*]

[1] Department of Cogno-Mechatronics Engineering, Pusan National University, Busan 46241, Korea; qkrtpwls314@pusan.ac.kr (S.J.P.); gh.kim@pusan.ac.kr (G.H.K.)
[2] Wellman Center for Photomedicine, Harvard Medical School and Massachusetts General Hospital, Boston, MA 02114, USA; HDLEE@mgh.harvard.edu
[3] Agency for Defense Development, Daejeon 305-150, Korea
*   Correspondence: ckim@pusan.ac.kr (C.-S.K.); minsjo@add.re.kr (M.J.)
†   These two authors contributed equally.

check for updates

Abstract: We demonstrate a novel narrow-linewidth configuration of a wavelength-swept active mode locking (AML) fiber laser. The frequency response of the modulation depth of a semiconductor optical amplifier can be improved in a higher modulation frequency region by adapting the cross gain modulation (XGM) configuration, compared to that of the conventional direct gain modulation (DGM) configuration. As a sufficient modulation depth is implemented for an AML at higher modulation frequencies at around gigahertz order, it results in a narrower linewidth of lasing output. For the same modulation frequency of 1361.25 MHz, the linewidth of 0.25 nm with DGM becomes narrower up to 0.113 nm with XGM, which corresponds to an improved point spread function with 1.41 mm of 6-dB roll-off.

1. Introduction

Over the last decade, the wavelength-swept laser has been used as a powerful tool in biomedical imaging and various sensing application areas [1–6]. In general, wavelength-swept lasers use wavelength-tunable filters with mechanical movements, such as Fabry-Perot tunable filters [1–3] and angle-scanning filters with diffraction gratings [4]. Recently, a few advanced designs of wavelength-swept lasers, such as Fourier-domain mode-locking lasers [5] and micro-electro-mechanical system (MEMS) tunable vertical-cavity surface-emitting lasers (VCSELs) [6], have shown high performances with fast sweep rates of over a few hundred kHz, wide bandwidths of over 100 nm, and narrow linewidths of under 0.1 nm, which are commonly required for optical coherence tomography (OCT) [7]. However, owing to the mechanical movement of their conventional wavelength tunable filters, such lasers inherently suffer from thermal and mechanical instabilities and nonlinear tuning problems [7–10]. Nowadays, wavelength-swept active mode locking (AML) lasers have been developed by exploiting a radio frequency (RF) signal generator to modulate the gain of a semiconductor optical amplifier (SOA) using an electric current pump directly, which can implement an output wavelength tuning from the AML condition matching in a chromatic dispersion cavity [8–10]. Wavelength-swept AML lasers have not only demonstrated sweep rates of over 100 kHz [8–10] and bandwidths of 100 nm [11] but have also shown a few particular advantages, such as higher duty ratios (> 90%), linear sweeping (>0.9999), and phase stability, due to their unique akinetic wavelength sweeping mechanism that eliminates conventional mechanical and sinusoidal movement [10,12]. However, wavelength-swept AML lasers have a critical drawback: a thick linewidth (larger than 0.25–0.61 nm) [8–10,13,14] compared to conventional

wavelength-swept lasers based on mechanical movement filters [1–6]. This means that one of the most critical challenges currently to use wavelength-swept AML lasers as a light source for practical applications is to reduce the linewidth [8–19].

It has been experimentally investigated that there is a tendency for reducing linewidth of the wavelength-swept AML lasers at higher modulation frequencies [15,16]. As a theoretical approach to this issue, a discrete model of wavelength-swept AML laser has been proposed recently to show that the AML matching conditions with both higher modulation frequency and higher dispersion cavity are helpful to induce a narrower spectral linewidth [17,18]. However, under the direct gain modulation (DGM) configuration used for most wavelength-swept AML laser schemes, this linewidth narrowing approach by increasing the modulation frequency is mostly limited below the region of a few hundred MHz. It has been experimentally shown that the lasing output cannot be built from the amplified spontaneous emission (ASE) spectra due to the modulation response degradation in a higher modulation frequency region. Because the carrier lifetime of an SOA is several hundreds of picoseconds, the modulation response of SOA is dramatically decreased at high frequencies around GHz range in a conventional DGM method wavelength-swept AML laser [20,21].

Meanwhile, it has been studied that the cross gain modulation (XGM) method can be used to modulate the optical gain by injecting intensity-modulated optical pump light into the SOA, instead of the conventional current-modulated electric pump injection into the SOA under the DGM configuration [22–26]. It is also known that the XGM can improve the frequency response of the modulation depth of the SOA by reducing the lifetime in the cavity [22,23]. In this study, we investigate the static and dynamic characteristics of the novel wavelength-swept laser by adapting the XGM method into the AML condition for the first time, as far as we know.

2. Experiments and Results

Before constructing a laser cavity, we tried to confirm experimentally that the XGM works better than the DGM in a high-frequency modulation condition. Figure 1a,b show the experimental setup to measure the modulation depth of the SOA in the DGM and XGM configurations, respectively. The modulation depth of the SOA (M_{SOA} = Ao/Ap) is newly defined as the ratio of the amplitude of the output electric signal modulation (Ao) compared to the amplitude of the pump electric signal modulation (Ap). The electrical output power from the light passing through a SOA (InPhenix, IPSAD1501) with C-band gain was measured using a 1-GHz bandwidth photodetector and an 8-GHz bandwidth electric spectrum analyzer (ESA) (Advantest, R3267). The amplified spontaneous emission (ASE) of another SOA (InPhenix, IPSAD1509) with a central wavelength of 1552.59 nm and power of 0.13 mW was used at the input port of the SOA. The modulation amplitude of the pump electric signal was set to 14 dBm and the initial frequency increased from 100 MHz to avoid the damage to the SOA due to low modulation frequency. In the DGM configuration in Figure 1a, the injected current of the SOA is directly modulated as a sinusoidal signal from a radio frequency signal generator (RF–SG) (Anritsu, 68369A/NV). A bias-T circuit was used to combine a DC current and an RF modulation signal prior to the position of the SOA. In the XGM configuration of Figure 1b, an external-cavity Littrow laser with a central wavelength of 1541.53 nm, a linewidth of ~100 kHz, and an output power of 1.38 mW was employed as the optical pump light into a series made up of a Mach-Zehnder modulator (MZM), a circulator, and a SOA. The modulation depth of the optical pump light was controlled with the modulation depth of the pump electric signal from the RF-SG. The direction of the optical pump light from the circulator (CIR1) port 1 to port 2 was opposite to the optical amplification signal light in the SOA gain part.

For both configurations shown in Figure 1a,b, it was observed that the modulation depth of the SOA decreased with increasing modulation frequency in a higher region over 100 MHz; however, the decreasing trends of modulation depth of the SOA were different for the modulation frequencies for both the configurations. Thus, the relative modulation depth of the SOA (M_{SOA}/M_i) is defined as the ratio of the modulation depth of the SOA at each modulation frequency compared to that at 0 MHz.
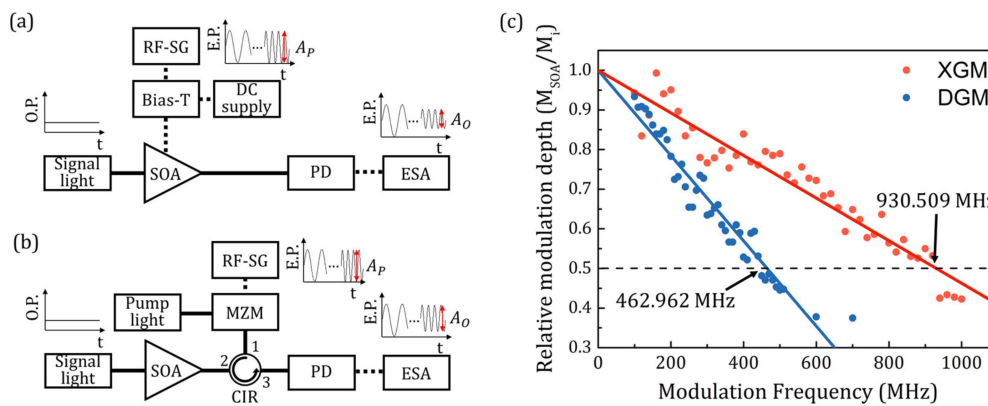
Figure 1. Experimental setup to measure the modulation depth of the semiconductor optical amplifier (SOA) (M_{SOA}) in (**a**) direct gain modulation (DGM) and (**b**) cross gain modulation (XGM). (**c**) Relative frequency response of the modulation depth of the SOA (M_{SOA}/M_i) for both DGM and XGM. E.P.: electrical power; O.P.: optical power; RF-SG: radio frequency signal generator; MZM: Mach-Zehnder modulator; ESA: electric spectrum analyzer; CIR: circulator; PD: photodetector; A_O: amplitude of output electric signal modulation; A_P: amplitude of pump electric signal modulation, M_i: modulation depth of SOA at 0 MHz.

Figure 1c shows the comparison of the relative frequency response of the modulation depth of the SOA for both the DGM and XGM cases. It is clearly shown that the frequency response of the modulation depth of the SOA decreases as the modulation frequency increases in both the DGM and XGM. The 3-dB points appeared at 462.962 and 930.509 MHz in the DGM and XGM, respectively. It means that the frequency response of the modulation depth of the SOA was enhanced by approximately two-fold by using the XGM.

Figure 2 shows the experimental set-up of the wavelength-swept AML laser based on the XGM configuration. The cavity consists of a SOA (InPhenix, IPSAD1501) acting as a gain medium, two optical circulators, three polarization controllers for optimizing the polarization states of the light propagating through the single mode optical fiber, an optical isolator to block the pump light to prevent undesired lasing, and a chirped fiber Bragg grating (CFBG) (TeraXion) acting as a dispersion medium (15 ps/nm at 1.5 μm) and an output coupler (reflectivity of ~60%). A 12.5 mW external-cavity Littrow laser was used as the optical pump light. The optical pump light was modulated by the MZM (iXblue, MX-LN-20) using a sinusoidal signal from the RF-SG. The intensity-modulated optical pump light was close to 4.1 mW due to the high loss of the MZM (−3.5 dB) at the 1.2-GHz modulation frequency. To achieve the high modulation depth of the SOA for the mode locking condition, a booster optical amplifier (BOA) (Aeon, Models CL) was inserted to increase the optical power of the intensity-modulated optical pump light at port 2 of the CIR2 up to 11 mW because it is well known that the extinction ratio of an SOA is improved by increasing the power of the pump light [22,23]. However, the power of the pump light needed to be controlled properly. In the case of the optical pump light being too strong, the gain of the SOA in the ring cavity cannot be fully increased to generate the laser output. The intensity-modulated optical pump light is injected through the circulator port 1 of CIR1 into the SOA in the direction opposite to the lasing signal. This injected pump light leads gain modulation of the SOA by depleting the gain of SOA. Therefore, the modulation depth of the SOA can be controlled via the modulation depth of the injected light. Moreover, the injected pump light reduces the carrier lifetime in the cavity due to stimulated recombination; high modulation frequency can be implemented. In this setup, an ASE of 0.2 mW comes out from the SOA in the cavity and acts as a signal light in the XGM configuration.
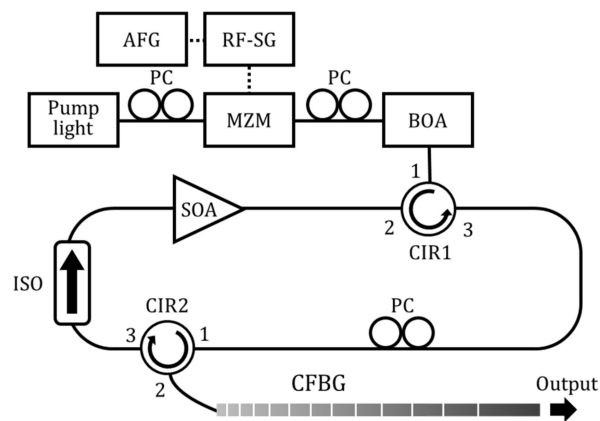
Figure 2. Experimental setup of the wavelength-swept active mode locking (AML) laser based on XGM. BOA: booster optical amplifier; ISO: optical isolator; CFBG: chirped fiber Bragg grating; PC: polarization controller; AFG: arbitrary function generator.

The wavelength of the optical pump light is another important parameter for a higher extinction ratio of the XGM. In general, the extinction ratio is maximized when the wavelength of the optical pump light is at the peak of the gain spectrum [21–24] and the peak of the gain spectrum is red-shifted when strong optical pump light is injected into the SOA due to the depletion of carriers [24,27]. However, setting the pump light at the center of gain spectrum causes excessive undesired lasing of optical pump light, which decreases the output power at the desired wavelength and the SNR. Therefore, the optical wavelength of the pump light was set to 1590.9 nm at the side of the gain spectrum and the measured extinction ratio was 7.5 dB.

A laser output with a short pulse train occurs when the modulation frequency matches the AML condition as follows [9]:

$$f_m = N \cdot FSR \tag{1}$$

where f_m is the modulation frequency applied to the SOA, N is the order of harmonic mode locking. The free spectral range of the laser cavity, *FSR*, is expressed as [9]:

$$FSR = \frac{c}{n_{eff}L} \tag{2}$$

where L is the cavity length, n_{eff} is the effective refractive index in the fiber ring cavity, and c is the speed of light in vacuum. The zero-order FSR, FSR_0, is driven from the cavity length and the speed of light in the fiber cavity [28,29]. However, since each wavelength has different AML conditions due to the dispersion medium of the CFBG, the deviation in the lasing wavelength, $\Delta\lambda_m$, is expressed as a function of the modulation frequency, f_m [9];

$$\Delta\lambda_m = -\frac{nL}{cD_{total}f_{m_0}}\Delta f_m \tag{3}$$

where $\Delta f_m = f_m\text{-}f_{m0}$, f_{m0} is the central mode-locking frequency, D_{total} is the dispersion parameter.

Figure 3a,b are examples of the spectral peak shape of static wavelength-swept AML laser at different mode-locking orders under the DGM and XGM configuration, respectively. For the central wavelength of 1574.1 nm and a cavity length of 3.752 m, FSR_0 is given as 54.45 MHz. Thus, the mode-locking orders, N, of 13, 17, 21, 25 correspond to the modulation frequencies, f_m, of 707.85, 925.65, 1143.45, 1361.25 MHz, respectively. We compared the linewidths of the XGM and DGM by applying the same RF signals with a different mode-locking order into the SOA directly or into the MZM for the same main cavity with the same FSR_0. In the DGM condition with the mode-locking frequencies higher than 707.85 nm for the 13th mode-locking order, it was observed that the linewidth tends to become broader as the frequency increases. However, the mode locking does not occur properly in

higher modulation frequency ranges because the relative frequency response of the modulation depth of the SOA deteriorates in the high mode-locking frequencies, as shown in Figure 1c. On the contrary, in the case of the XGM, the linewidth gradually decreased as the modulation frequency increased over 707.85 MHz. The linewidth, defined as a 3-dB spectral width, was 0.119 nm for the XGM, but it was 1.291 nm for DGM, at a modulation frequency of 1361.25 MHz of the 25th mode-locking order. Inset of Figure 3b shows the relationship between the linewidth and modulation frequency under the XGM condition. Thus, we can experimentally confirm that the enhanced frequency response of the modulation depth of the SOA by using the XGM was indeed helpful to achieve a narrower linewidth of the AML laser output.
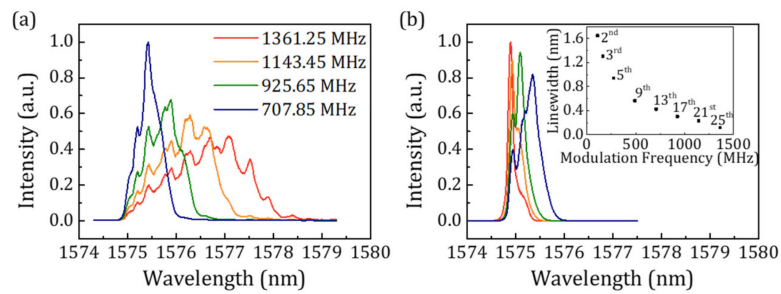

Figure 3. Comparison of the output spectra at the 13rd, 17th, 21st, and 25th orders of mode locking of (**a**) DGM and (**b**) XGM. Inset: Relationship between the linewidth and modulation frequency of XGM.

Figure 4a shows the tuning of the output spectra of the wavelength-swept AML laser. For a cavity length of 10.27 m and the corresponding FSR_0 of 19.89 MHz, the modulation frequencies around 850 MHz are matched to the mode-locking order of 43. The intensity of the optical pump light measured at port 2 of CIR1 was 7.2 mW for an injection current of 301.9 mA. As the modulation frequency, fm, increased from 844.77 to 855.3 MHz, the lasing wavelength λm shifted from 1551.05 to 1589.45 nm. The sensitivity was 3.64 nm/MHz. Undesired lasing at 1590.9 nm was also observed, which was caused by the optical pump light reflected from the SOA. The intensity difference between the signal light and optical pump light was around 18 dB. The linewidth and intensity of the laser varied depending on the wavelength, but there was no significant difference within the tuning range. The signal to noise ratio (SNR) was measured over 35 dB in most of tuning region. As shown in Figure 4b, the average linewidth of the laser was 0.112 nm and the narrowest linewidth was 0.086 nm at the central wavelength of 1559.7 nm for the modulation frequency of 847.11 MHz. Figure 4b also shows the linearity of the wavelength-swept AML laser based on the XGM with the R-squared value of 0.99997.
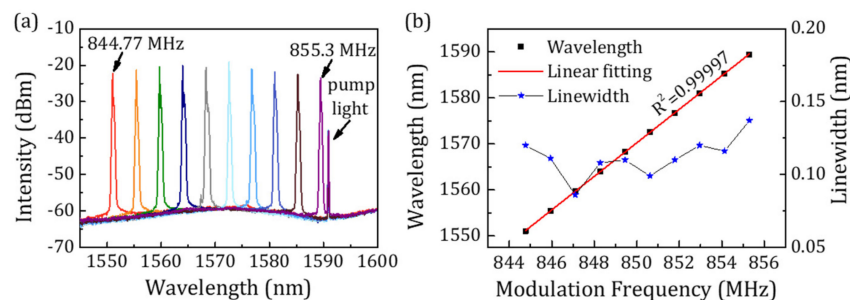

Figure 4. (**a**) Static spectra of the wavelength-swept AML laser based on the XGM. (**b**) Mode locked wavelength (left y axis) and linewidth (right y axis) versus modulation frequency.

To measure the dynamic characteristics of the XGM, the spectrum was measured while sweeping the modulation frequency. For high linearity and a high duty cycle, a negative saw-tooth waveform from an arbitrary function generator (AFG) (Tektronix, AFG3022C) was externally applied to a frequency modulation (FM) port of the RF-SG to sweep the modulation frequency. Figure 5a shows the peak-hold

spectra at a sweeping rate at 100 kHz, and the 6-dB tuning bandwidth was measured to be 41.25 nm; this result is in good agreement with the 3-dB optical bandwidth of the SOA, which was ~45 nm. Figure 5b shows the temporal series of the laser output, measured with 350 MHz photodetector (PD) (Thorlabs, PDB430C-AC).
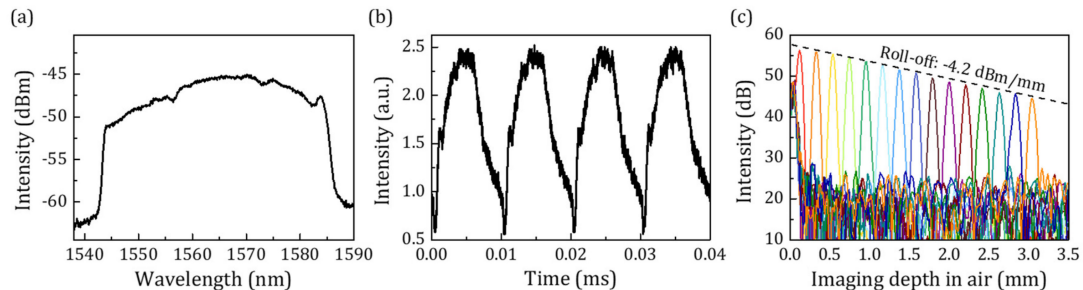

Figure 5. (**a**) Wavelength sweeping spectra on peak-hold mode. (**b**) Temporal shape of the sweeping spectra at a sweeping rate of 100 kHz. (**c**) Point spread function at different imaging depths.

The dynamic characteristics were evaluated based on a 6-dB roll-off of the point spread function (PSF), which was acquired through the Fourier transform of an interference signal by passing through a fiber-type Mach–Zehnder interferometer (MZI). Figure 5c shows the measured sweeping trace of a sawtooth wave drive function at 20 kHz. This 6-dB PSF parameter using the XGM was measured as 1.41 mm.

3. Conclusions

We demonstrated a narrower linewidth wavelength-swept AML laser based on the XGM configuration. The 3-dB point of the frequency response of SOA was improved approximately two-fold in XGM compared to that of DGM. The experimental results show that the linewidth is narrowed with increasing the mode locking frequency based on XGM. Due to enhanced frequency response, the wavelength-swept laser based on XGM successfully worked at 1361.25 MHz modulation frequency and was measured as 0.113 nm, which is much narrower than that of DGM with 0.25 nm. The proposed laser also showed properties of high linearity, high SNR, and sweep rate of 100 kHz, in addition to the narrower linewidth. This study proposes a novel method that can overcome one of the disadvantages, the broad linewidth, of wavelength-swept AML lasers for practical applications.

Author Contributions: G.H.K. designed the experiments; S.J.P. and G.H.K. constructed the experimental setup; C.-S.K. and H.D.L. confirmed the experiments; S.J.P. and G.H.K. obtained and analyzed the data; S.J.P., G.H.K., H.D.L., M.J., and C.-S.K. discussed the experimental results; S.J.P., G.H.K., H.D.L., M.J., and C.-S.K. contributed to writing and reviewing the paper.

Conflicts of Interest: The authors declare no conflict of interest.

References

1. Yun, S.H.; Richardson, D.J.; Culverhouse, D.O.; Kim, B.Y. Wavelength-Swept fiber laser with frequency shifted feedback and resonantly swept intra-Cavity acoustooptic tunable filter. *IEEE J. Sel. Top. Quantum Electron.* **1997**, *3*, 1087–1096. [CrossRef]
2. Huber, R.; Wojtkowski, M.; Fujimoto, J.G. Fourier Domain Mode Locking (FDML): A new laser operating regime and applications for optical coherence tomography. *Opt. Express* **2006**, *14*, 3225. [CrossRef] [PubMed]
3. Jung, E.J.; Kim, C.S.; Jeong, M.Y.; Kim, M.K.; Jeon, M.Y.; Jung, W.; Chen, Z. Characterization of FBG sensor interrogation based on a FDML wavelength swept laser. *Opt. Express* **2008**, *16*, 16552–16560. [PubMed]

4. Oh, W.; Vakoc, B.J.; Shishkov, M.; Tearney, G.J.; Bouma, B.E. >400 kHz repetition rate wavelength-Swept laser and application to high-Speed optical frequency domain imaging. *Opt. Lett.* **2010**, *35*, 2919. [CrossRef] [PubMed]

5. Wieser, W.; Klein, T.; Adler, D.C.; Trépanier, F.; Eigenwillig, C.M.; Karpf, S.; Schmitt, J.M.; Huber, R. Extended coherence length megahertz FDML and its application for anterior segment imaging. *Biomed. Opt. Express* **2012**, *3*, 2647. [CrossRef] [PubMed]

6. Tsai, T.H.; Potsaid, B.; Tao, Y.K.; Jayaraman, V.; Jiang, J.; Heim, P.J.S.; Kraus, M.F.; Zhou, C.; Hornegger, J.; Mashimo, H.; et al. Ultrahigh speed endoscopic optical coherence tomography using micromotor imaging catheter and VCSEL technology. *Biomed. Opt. Express* **2013**, *4*, 1119. [CrossRef] [PubMed]

7. Klein, T.; Huber, R. High-Speed OCT light sources and systems. *Biomed. Opt. Express* **2017**, *8*, 828. [CrossRef] [PubMed]

8. Lee, H.D.; Lee, J.H.; Jeong, M.Y.; Kim, C.S. Characterization of wavelength-Swept active mode locking fiber laser based on reflective semiconductor optical amplifier. *Opt. Express* **2011**, *19*, 14586.

9. Lee, H.D.; Jeong, M.Y.; Kim, C.S.; Jun Geun, S.; Lee, B.H.; Eom, T.J. Linearly Wavenumber-Swept Active Mode Locking Short-Cavity Fiber Laser for In-Vivo OCT Imaging. *IEEE J. Sel. Top. Quantum Electron.* **2014**, *20*, 433–440.

10. Lee, H.D.; Kim, G.H.; Eom, T.J.; Jeong, M.Y.; Kim, C.S. Linearized Wavelength Interrogation System of Fiber Bragg Grating Strain Sensor Based on Wavelength-Swept Active Mode Locking Fiber Laser. *J. Lightwave Technol.* **2015**, *33*, 2617–2622. [CrossRef]

11. Yamashita, S.; Asano, M. Wide and fast wavelength-tunable mode-locked fiber laser based on dispersion tuning. *Opt. Express* **2006**, *14*, 9399. [CrossRef] [PubMed]

12. Lee, H.D.; Kim, G.H.; Shin, J.G.; Kim, C.S.; Eom, T.J. Retinal OCT imaging based on actively mode locked akinetic swept source at 1080 nm wavelength (Conference Presentation). In Proceedings of the Optical Coherence Tomography and Coherence Domain Optical Methods in Biomedicine XXIII, San Francisco, CA, USA, 4 March 2019; p. 6.

13. Nakazaki, Y.; Yamashita, S. Fast and wide tuning range wavelength-Swept fiber laser based on dispersion tuning and its application to dynamic FBG sensing. *Opt. Express* **2009**, *17*, 8310. [CrossRef] [PubMed]

14. Yamashita, S.; Takubo, Y. Wide and fast wavelength-Swept fiber lasers based on dispersion tuning and their application to optical coherence tomography. *Photonic Sens.* **2013**, *3*, 320–331. [CrossRef]

15. Stancu, R.F.; Podoleanu, A.G. Dual-mode-locking mechanism for an akinetic dispersive ring cavity swept source. *Opt. Lett.* **2015**, *40*, 1322. [CrossRef] [PubMed]

16. Stancu, R.F.; Podoleanu, A.G. Short ring cavity swept source based on a highly reflective chirped FBG. *Photonic Sens.* **2015**, *5*, 251–256. [CrossRef]

17. Burgoyne, B.; Dupuis, A.; Villeneuve, A. An Experimentally Validated Discrete Model for Dispersion-Tuned Actively Mode-Locked Lasers. *IEEE J. Sel. Top. Quantum Electron.* **2014**, *20*, 390–398. [CrossRef]

18. Zhang, C.; Liao, P.; Burgoyne, B.; Kim, Y.; Trepanier, F.; Villeneuve, A.; Liboiron-Ladouceur, O. Low-Cost Dispersion-Tuned Active Harmonic Mode-Locked Laser with a 3-cm Coherence Length. *IEEE J. Sel. Top. Quantum Electron.* **2014**, *20*, 399–405. [CrossRef]

19. Hasegawa, Y.; Shirahata, T.; Yamashita, S. Analysis of Dynamic Properties of Dispersion-Tuned Swept Lasers. *J. Lightwave Technol.* **2015**, *33*, 219–226. [CrossRef]

20. Mork, J.; Mecozzi, A.; Eisenstein, G. The modulation response of a semiconductor laser amplifier. *IEEE J. Sel. Top. Quantum Electron.* **1999**, *5*, 851–860. [CrossRef]

21. Mork, J.; Nielsen, M.L.; Berg, T.W. The Dynamics of Semiconductor Optical Amplifiers: Modeling and Applications. *Opt. Photonics News* **2003**, *14*, 42. [CrossRef]

22. Jin, X.; Keating, T.; Chuang, S.L. Theory and experiment of high-Speed cross-gain modulation in semiconductor lasers. *IEEE J. Quantum Electron.* **2000**, *36*, 1485–1493. [CrossRef]

23. Obermann, K.; Kindt, S.; Breuer, D.; Petermann, K. Performance analysis of wavelength converters based on cross-gain modulation in semiconductor-optical amplifiers. *J. Lightwave Technol.* **1998**, *16*, 78–85. [CrossRef]

24. Chang, Y.C.; Hung, C.M.; Yu, K.C.; Lin, G.R. Optimization on cross-gain-modulating power and wavelength for pulsed data-pattern reshaping in optical-clock controlled semiconductor optical amplifier. In Proceedings of the 2006 Optical Fiber Communication Conference and the National Fiber Optic Engineers Conference, Anaheim, CA, USA, 5–10 March 2006; pp. 57–59.

25. Joergensen, C.; Danielsen, S.L.; Stubkjaer, K.E.; Schilling, M.; Daub, K.; Doussiere, P.; Pommerau, F.; Hansen, P.B.; Poulsen, H.N.; Kloch, A.; et al. All-optical wavelength conversion at bit rates above 10 Gb/s using semiconductor optical amplifiers. *IEEE J. Sel. Top. Quantum Electron.* **1997**, *3*, 1168–1180. [CrossRef]

26. Chelles, S.; Devaux, F.; Meichenin, D.; Sigogne, D.; Carenco, A. Extinction ratio of cross-gain modulated multistage wavelength converters: Model and experiments. *IEEE Photonics Technol. Lett.* **1997**, *9*, 758–760. [CrossRef]

27. Henning, I.; Adams, M.; Collins, J. Performance predictions from a new optical amplifier model. *IEEE J. Quantum Electron.* **1985**, *21*, 609–613. [CrossRef]

28. Park, S.M.; Park, S.Y.; Kim, C.S. Comb-Spacing-Swept Source Using Differential Polarization Delay Line for Interferometric 3-Dimensional Imaging. *Curr. Opt. Photonics* **2019**, *3*, 16–21.

29. Lee, Y.W.; Jung, J. Characterization of a Tunable Flattened-Pass-Band Fiber Comb Filter. *Curr. Opt. Photonics* **2019**, *3*, 111–118.